Focusing of elliptically polarized Gaussian beams through an annular high numerical aperture*

Chen Bao-Suan(陈宝算) and Pu Ji-Xiong(蒲继雄)†

Department of Information Science & Engineering, Huaqiao University, Quanzhou 362021, *China*

(Received 15 November 2009; revised manuscript received 24 December 2010)

Based on the vectorial Debye theory, the focusing properties of the Gaussian beam through an annular high numerical aperture are studied numerically, including the intensity, the phase and the orbital angular momentum properties. Then the influence of certain parameters on the focusing properties is also investigated. It is shown that sub-wavelength elliptical light spots can be obtained. And there exists a vortex in the longitudinal component of the focused field even though the incident beam is Gaussian beam, indicating that the spin angular momentum of the elliptically polarized Gaussian beam is converted into the orbital angular momentum by the focusing.

Keywords: Debye theory high numerical aperture, elliptically polarized, focusing
PACC: 4225, 4225F, 4290

1. Introduction

The focusing of a laser beam through a high numerical-aperture(NA) objective will produce sub-wavelength focal spots.[1−3] In 2007, Grosjean discussed the smallest focal spots obtained in different conditions by use of tight focusing systems.[4] It is known to all that after being tightly focused, the incident beam is depolarized and a longitudinal component is created near the focus, thus three-dimensional spatial resolution can be increased by the tight focusing system.[3,5,6] Due to its unique properties, the tight focusing systems can be applied in many fields, such as microscopy, lithography, optical data storage, optical trapping, electron acceleration and plasma physics.[7−12] On the other hand, angular momentum contains both spin angular momentum (SAM) and orbital angular momentum (OAM).[13] Laser beams that carry OAM have many applications in such areas as micro machines, optical spanners, and quantum information encodinig etc.[14] In recent years, many researchers have extensively studied the distribution and measurement of OAM.[15−20] In the present paper, we study the tight focusing properties of an elliptically polarized Gaussian beam through an annular aperture based on the vectorial Debye theory.[21] It is shown that an SAM of the beam can be converted into an OAM near the focus.

2. Theory

The focusing system studied in this paper is shown in Fig. 1. The incident beam is considered to be a Gaussian beam, which can be expressed as

$$E(r) = E_0 \exp(-r^2/w_0^2), \tag{1}$$

where E_0 and w_0 are the constants representing the amplitude and beam waist of the Gaussian beam respectively. The Gaussian beam is a kind of non-vortex beam without a helical phase factor, indicating that there is no initial OAM with it.

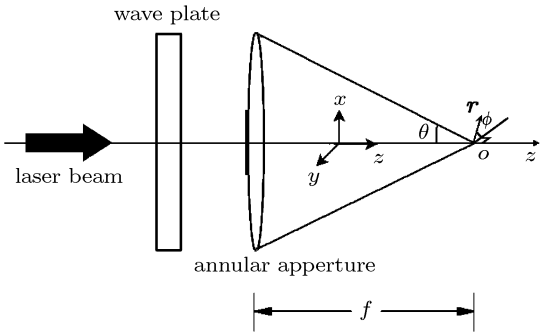


Fig. 1. Schematic diagram of tight focusing.

Then, we consider the incident beam to be an elliptically polarized Gaussian beam, which can be described by the superposition of two orthogonal linearly

*Project supported by the National Natural Science Foundation of China (Grant No. 60977068), and the Natural Science Foundation of Fujian Province, China (Grant No. A0810012).
†Corresponding author. E-mail: jixiong@hqu.edu.cn
© 2010 Chinese Physical Society and IOP Publishing Ltd

polarized beams as

$$E_{\pm}(r) = E_x \boldsymbol{e}_x \pm E_y \mathrm{e}^{\mathrm{i}\,\beta} \boldsymbol{e}_y, \tag{2}$$

in which β is the retardation between the two beams; $E_+(r)$ and $E_-(r)$ represent the right-hand elliptically (RHE) polarized and the left-hand elliptically (LHE) polarized beams respectively; $\boldsymbol{e}_x$ and $\boldsymbol{e}_y$ are unit vectors along the x and the y directions.

Under sine condition, the high NA objective of the focusing system follows $r = f\sin\theta$, where f is the focal length of the objective. Then the pupil apodization function after the lens can be written as

$$\begin{aligned} A_{\pm}(\theta) \;=\; & E_{0x} \exp\left(-\frac{f^2 \sin^2\theta}{w_0^2} \right) \boldsymbol{e}_x \\ & \pm E_{0y} \exp(\mathrm{i}\,\beta) \exp\left(-\frac{f^2 \sin^2\theta}{w_0^2} \right) \boldsymbol{e}_y. \end{aligned} \tag{3}$$

For simplicity, we consider only the x-polarized component here, and the y-polarized component can be written similarly. Then the field in the focal region when the x-polarized Gaussian beam is focused by an annular high NA objective can be obtained according to the vectorial Debye theory as follows:[21−23]

$$E(r,\phi,z) = \begin{bmatrix} E_x \\ E_y \\ E_z \end{bmatrix} = \frac{\pi\,\mathrm{i}}{x} \begin{bmatrix} I_0 + \cos(2\phi) I_2 \\ \sin(2\phi) I_2 \\ 2\,\mathrm{i}\cos(\phi) I_1 \end{bmatrix}, \tag{4}$$

where (r,ϕ,z) is the cylindrical coordinates of an observation point, E_x, E_y and E_z are the three components of the observation point in the focal region, indicating that the x-polarized Gaussian beam is depolarized by the focusing. And I_0, I_1 and I_2 are given as[23]

$$I_0(r,z) = \int_{\theta_{\min}}^{\theta_{\max}} A(\theta)\sqrt{\cos\theta}\sin\theta(1+\cos\theta) J_0(kr\sin\theta)\exp(\mathrm{i}\,kz\cos\theta)\mathrm{d}\theta, \tag{5}$$

$$I_1(r,z) = \int_{\theta_{\min}}^{\theta_{\max}} A(\theta)\sqrt{\cos\theta}\sin^2\theta J_1(kr\sin\theta)\exp(\mathrm{i}\,kz\cos\theta)\mathrm{d}\theta, \tag{6}$$

$$I_2(r,z) = \int_{\theta_{\min}}^{\theta_{\max}} A(\theta)\sqrt{\cos\theta}\sin\theta(1-\cos\theta) J_2(kr\sin\theta)\exp(\mathrm{i}\,kz\cos\theta)\mathrm{d}\theta, \tag{7}$$

where $\theta_{\min}$ and $\theta_{\max}$ are the minimum and the maximum numerical angles of the annular aperture determined by $\mathrm{NA}_{\min}$ and $\mathrm{NA}_{\max}$respectively.

We then turn to studying the OAM of the Gaussian beam in the focused field. Since the beam is passing through an annular high NA objective, the OAM should be analysed under the nonparaxial condition suggested by Refs. [14], [24], and [25]. In this case, the OAM of the Gaussian beam in the focused field can be expressed as

$$L_z = \frac{\sigma}{\omega} \left\{ 1 + \frac{\int_{\kappa_{\min}}^{\kappa_{\max}} \mathrm{d}\kappa [|E(\kappa)|^2 \kappa/(k^2-\kappa^2)]}{\int_{\kappa_{\min}}^{\kappa_{\max}} \mathrm{d}\kappa [|E(\kappa)|^2 (2k^2-\kappa^2)/\kappa(k^2-\kappa^2)]} \right\} W, \tag{8}$$

where σ and ω are the helicity and the frequency of the light beam: when $\sigma = 0$ the beam is linearly polarized and when $\sigma = \pm 1$ the beam is circularly polarized; $\kappa = k\sin\theta$ is the special frequency related to numerical angle θ; W is the total energy of the beam in the focused field which is obtained from

$$W = -\varepsilon_0 \int_{-\infty}^{\infty} \int_0^{2\pi} |E(r,\phi,z)|^2 r \mathrm{d}r\mathrm{d}\phi \tag{9}$$

with ε_0 being the permittivity of vacuum.

With the above derived equations, the intensity, the phase and the OAM in the focused field can be investigated.

3. Results

The focusing properties of the elliptically polarized Gaussian beam through an annular high NA objective are investigated in this section. The focusing intensities of the RHE polarized and the LHE polarized beams are given in Fig. 2 separately. It is shown that elliptical focal spots are obtained. The difference in focusing between the RHE polarized beam and LHE polarized beam is in the direction of the major axis of the elliptic spots. It is also found that the distribution of the z component splits into two parts.

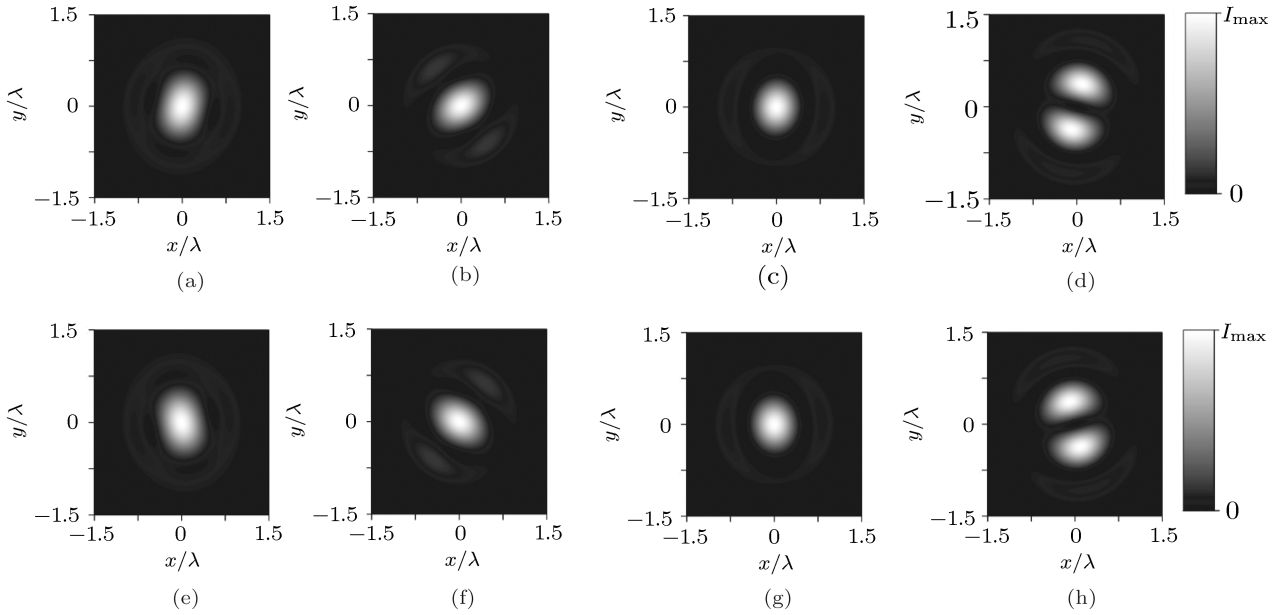


Fig. 2. Intensity distributions in the focal plane for RHE polarized and LHE polarized Gaussian beams (a)–(d) RHE polarized beam; (e)–(h) LHE polarized beam; (a) and (e)total intensity; (b) and (f) x component intensity; (c) and (g) y component intensity; (d) and (h) z component intensity. The other parameters are chosen as $\lambda = 632.8$ nm, $\mathrm{NA}_{\min} = 0.3$, $\mathrm{NA}_{\max} = 0.95$, $w = 1.5$ cm, $f = 1$ cm, $\beta = \pi/4$, $E_{0x} = 1$, and $E_{0y} = 3$.

Figure 3 shows the corresponding phase contours for the x, y and z components of both RHE polarized and LHE polarized beams. It is found from Figs. 3(a), 3(b), 3(d), and 3(e) that the central phases of x and y components keep invariant. That is because the Gaussian beam is a type of non-vortex beam. However, it is obvious from Figs. 3(c) and 3(f) that there exists a helical phase distribution in the z component, which explains why the z component splits into two parts. The helical phase distribution indicates that the longitudinal component created by tight focusing carries OAM, which means that by tight focusing, the SAM of the elliptically polarized Gaussian beam can be converted into the OAM.

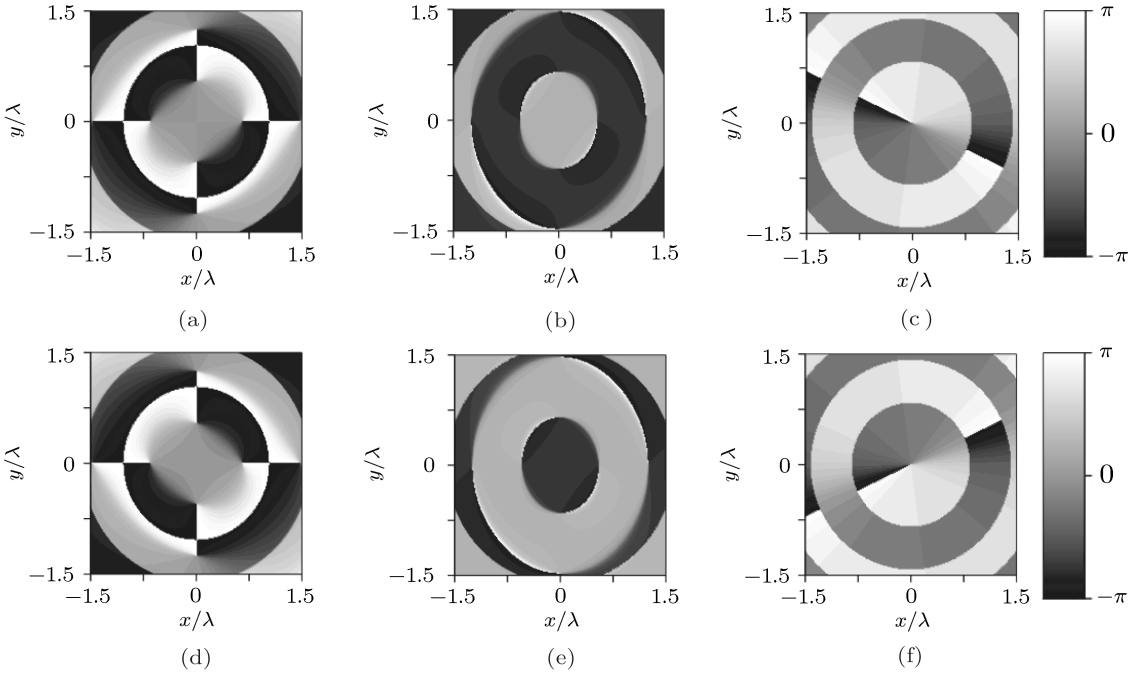


Fig. 3. Phase contours of x, y and z components in the focal plane. (a), (b) and (c) RHE polarized beam; (d), (e) and (f) LHE polarized beam; (a) and (d) $E_x(r, \phi, z)$; (b) and (e) $E_y(r, \phi, z)$; (c) and (f) $E_z(r, \phi, z)$. The other parameters are the same as those in Fig. 2.

Since the created longitudinal component exhibits more specific characteristics, we then focus our study on the influence of certain parameters on the intensity and the phase distributions of the z component in the focal field. The influence of E_{0y} is shown in Fig. 4. It is found that with the increase of E_{0y}, the spot shape of the z component will rotate in an anticlockwise direction, while the helical phase distribution will rotate in a clockwise direction. When $E_{0y} = 25 \gg E_{0x}$, i.e. the incident Gaussian beam can be regarded as being linearly polarized in the y direction, then the longitudinal spot keeps upright as shown in Fig. 4(d). Moreover, it is shown in Fig. 4(h) that there is no helical phase distribution in the longitudinal component when $E_{0y} = 25$, indicating that the z component carries no OAM. That is because no SAM could be converted into OAM when the incident beam is linearly polarized.

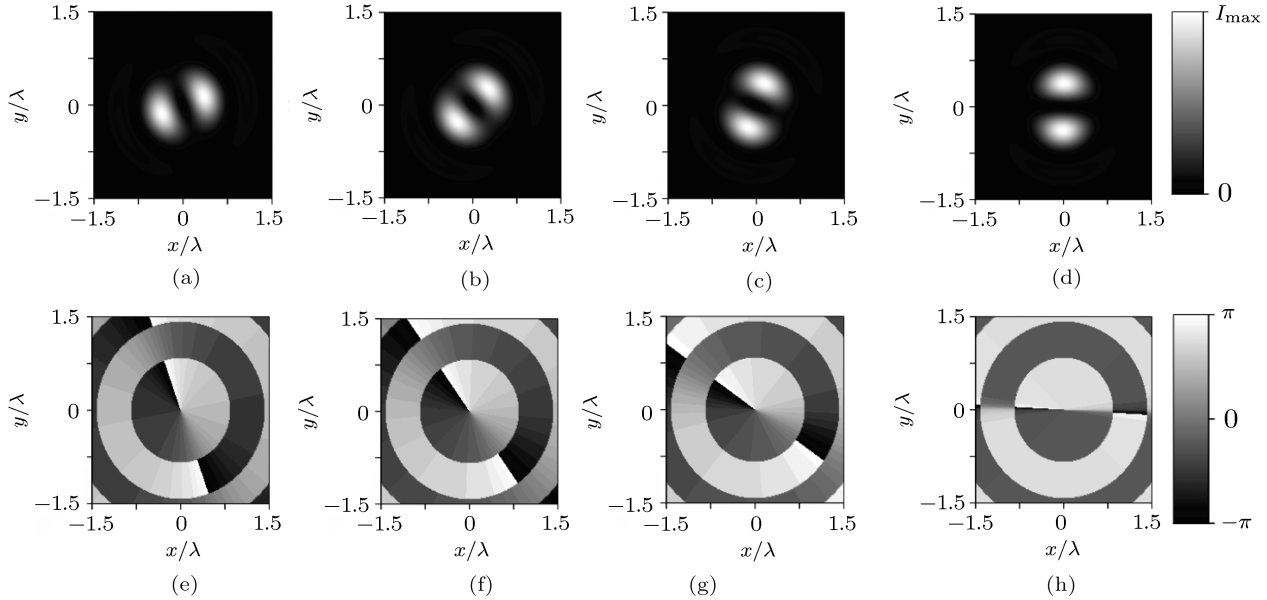


Fig. 4. Influence of E_{0y} on longitudinal intensity and phase distribution in the focal plane. (a)–(d) Intensity distribution; (e)–(h) phase distribution; (a) and (e) $E_{0y} = 0.5$; (b) and (f) $E_{0y} = 1$; (c) and (g) $E_{0y} = 2$; (d) and (h) $E_{0y} = 25$. The other parameters are the same as those in Fig.2.

The intensity and the phase distributions of the z component with different values of retardation β are shown in Fig. 5.

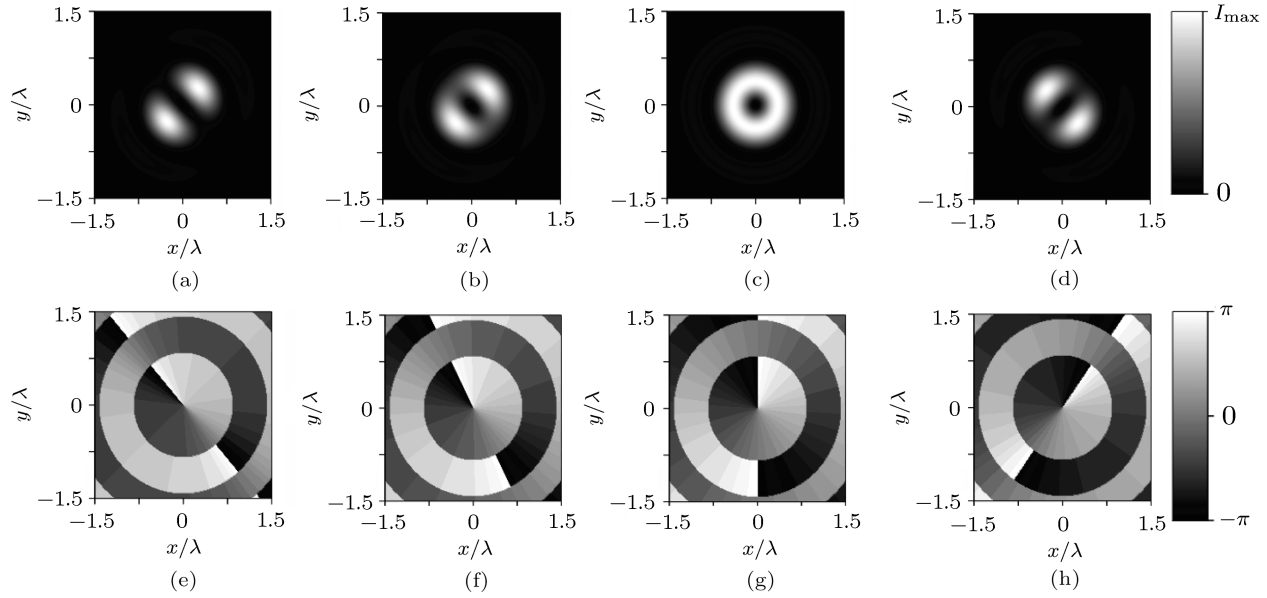


Fig. 5. Influence of β on longitudinal intensity and phase distribution in the focal plane. (a)–(d) Intensity distribution; (e)–(h) phase distribution; (a) and (e) $\beta = \pi/6$; (b) and (f) $\beta = \pi/3$; (c) and (g) $\beta = \pi/2$; (d) and (h) $\beta = 3\pi/4$. $E_{0y} = 1$. The other parameters are the same as those in Fig.2 except the varying one.

The intensity of the z component exhibits two separate spots when $\beta = \pi/6$ as shown in Fig. 5(a). As β increases, the two separate spots disperse and gradually form a circular hollow spot when $\beta = \pi/2$. As β further increases, the spot splits back into two separate parts again, but with the major axis of the elliptical spots in a different direction. The corresponding phase variation is shown in Figs. 5(e)–5(h). It is found that the position of the helical phase distribution will rotate with the increase of retardation β. When $\beta = \pi/2$, the dislocation line of the vortex is upright (see Fig. 5(g)).

Then the influence of the inner NA of the annular aperture $\mathrm{NA_{min}}$ on the intensity and the phase distribution of the longitudinal component is shown in Fig. 6. It is found that the intensity distribution keeps invariant as $\mathrm{NA_{min}}$ increases except that the beam spot becomes smaller. From Figs. 6(e)–6(h), it is also found that the corresponding vortex becomes smaller as well, indicating that the transverse field is focused into a tighter spot as $\mathrm{NA_{min}}$ increases.

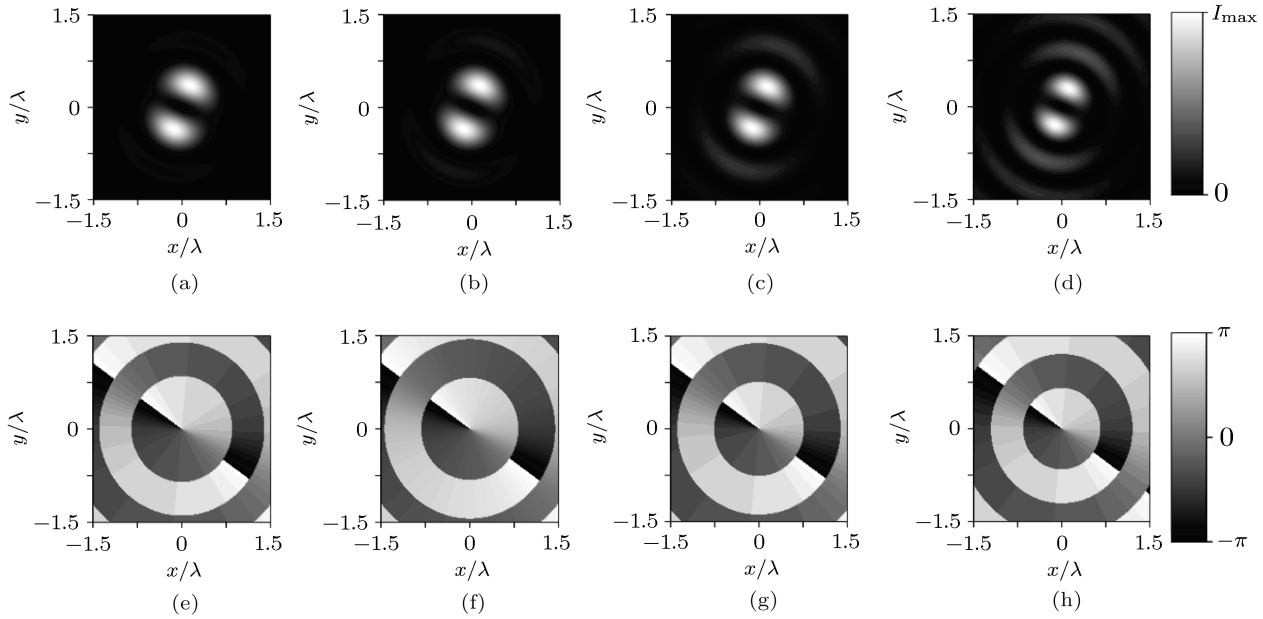
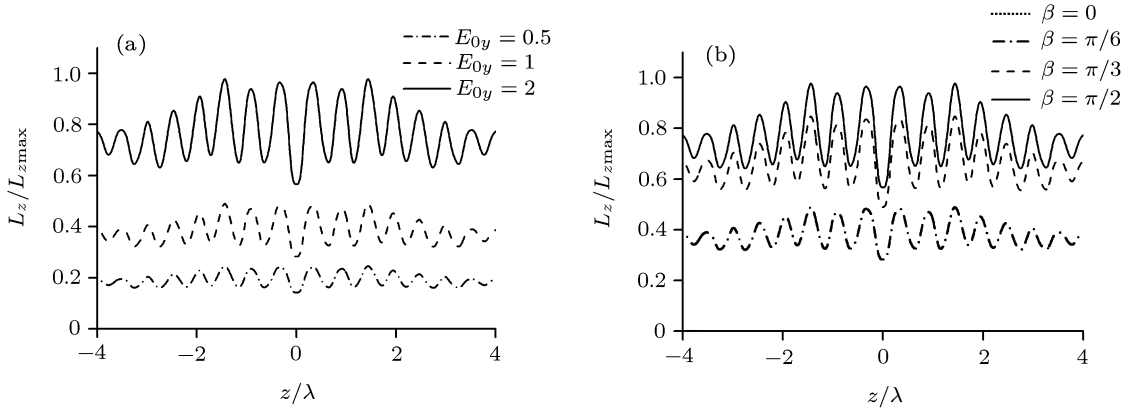


Fig. 6. Influence of $\mathrm{NA_{min}}$ on longitudinal intensity and phase distribution in the focal plane. (a)–(d) Intensity distribution; (e)-(h)phase distribution; (a) and (e) $\mathrm{NA_{min}} = 0.1$; (b) and (f) $\mathrm{NA_{min}} = 0.4$; (c) and (g) $\mathrm{NA_{min}} = 0.6$; (d) and (h) $\mathrm{NA_{min}} = 0.9$. $E_{0y} = 2$. The other parameters are the same as those in Fig.2 except the varying one.

The OAM variations with E_{0y}, β and $\mathrm{NA_{min}}$ while focusing are then illustrated in Fig. 7. From Fig. 7(a), it is found that the OAM increases with the increase of E_{0y}. It is shown from Eq. (8) that the OAM is proportional to the energy of the beam. And the increase of E_{0y} will increase the total energy of the beam which results in the increase of the OAM.



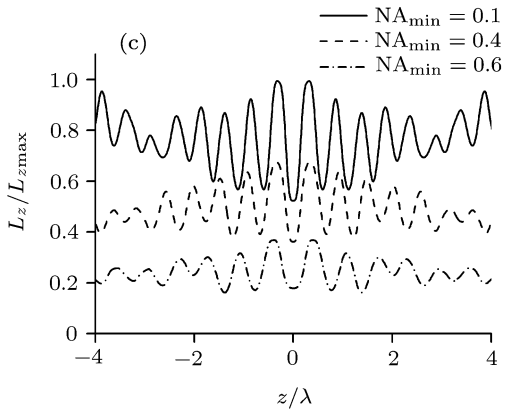


Fig. 7. Influence of (a) E_{0y}, (b) β ($E_{0y} = 2$), and (c) $\mathrm{NA_{min}}$ ($E_{0y} = 2$) on OAM distribution. The other parameters are the same as those in Fig. 2 except for the varying ones.

It is found from Fig. 7(b) that when $\beta = 0$, the incident beam becomes linearly polarized and the SAM of the beam equals zero, thus no OAM is obtained in the focusing. Moreover, as β increases from zero to $\pi/2$, the incident beam gradually changes from linearly polarized into circularly polarized and the SAM of the incident beam gradually increases, leading to the increase of OAM. Then from Fig. 7(c), we find that the OAM decreases with the increase of $\mathrm{NA_{min}}$, which is attributed to the energy decrease of the beam with the increase of $\mathrm{NA_{min}}$.

4. Conclusions

The focusing of elliptically polarized Gaussian beams through an annular high numerical aperture is investigated based on the vectorial Debye theory. It is found that elliptical spots can be obtained by focusing, and the spot will rotate by adjusting certain parameters. Thus the tight focusing technique can be used as a method of shaping beams. Then the OAM distribution while focusing is also investigated. It is found that the OAM is related to the SAM and the energy of the incident beam and the numerical aperture of the focusing objective also contributes to the OAM distribution. The results may have potential applications in optical spanners, particle manipulation, etc.

References

[1] Zhan Q 2007 *Opt. Lett.* **31** 867
[2] Dorn R, Quabis S and Leuchs G 2003 *Phys. Rev. Lett.* **91** 233901
[3] Zhang Z, Pu J and Wang X 2008 *Opt. Lett.* **33** 49
[4] Grosjean T and Courjon D 2007 *Opt. Commun.* **272** 314
[5] Hayazawa N, Saito Y and Kawata S 2004 *Appl. Phys. Lett.* **85** 6239
[6] Bokor N and Davidson N 2007 *Opt. Commun.* **279** 229
[7] Walker E P and Milster T D 2001 *Proc. SPIE Int. Soc. Opt. Eng.* **4443** 73
[8] Helseth L E 2002 *Opt. Commun.* **212** 343
[9] Efimenko E S, Kim A V and Quirogo-Teixeiro M 2009 *Phys. Rev. Lett.* **102** 015002
[10] Chen M, Sheng Z M and Zhang J 2005 *Chin. Phys.* **14** 1407
[11] Chen M, Sheng Z M and Zhang J 2006 *Chin. Phys.* **15** 568
[12] He F, Yu W, Lu P X, Yuan X and Liu J R 2004 *Acta Phys. Sin.* **53** 165 (in Chinese)
[13] Terriza G M, Torres J P and Torner L 2003 *Opt. Commun.* **228** 155
[14] Barnett S M and Allen L 1994 *Opt. Commun.* **110** 670
[15] Kotlyar V V, Khonina S N, Skidanov R V and Soifer V A 2007 *Opt. Commun.* **274** 8
[16] Soskin M S, Gorshkov V N, Vasnetsov M V, Malos J T and Heckenberg N R 1997 *Phys. Rev.* A **56** 4064
[17] Bomzon Z, Gu M and Shamir J 2006 *Appl. Phys. Lett.* **89** 241104
[18] Roux F S 2004 *Opt. Commun.* **242** 45
[19] Allen L and Padgett M J 2000 *Opt. Commun.* **184** 67
[20] Courtial J and Padgett M J 1999 *Opt. Commun.* **173** 269
[21] Gu M 2000 *Advanced Optical Imaging Theory* (Heidelberg: Springer)
[22] Richards B and Wolf E 1959 *Proc. R. Soc. London* Ser. A **253** 358
[23] Bomzon Z and Gu M 2007 *Opt. Lett.* **32** 3017
[24] Soskin M S and Vasnetsov M V In: Wolf E 2001 *Progress in Optics* (Amsterdam: Elsevier) **42** 219
[25] Zhang Z, Pu J and Wang X 2008 *Opt. Eng.* **47** 068001